A *GUI* for the Synthesis and Design of Analog Filters based on Pascal and other Classical Approximations

Víctor H. Hernández-Juárez, Luis A. Sánchez-Gaspariano, Carlos Sánchez-López, Richard Torrealba-Meléndez, Jesús M. Muñoz-Pacheco, Carlos Muñiz-Montero, and Luz del Carmen Gómez-Pavón

***Abstract*—A *Graphical User Interface* (*GUI*) called SAFIMAM (acronym of Synthesis of Analog Filters in MATLAB by Approximation Methods) developed in MATLAB App Designer, an interactive development environment for designing an app layout and programming its behavior, capable of carrying out the synthesis of analog filters based on classical approximation methods as well as the Pascal approach, starting from a few design specifications, is presented. Quantitative metrics regarding computational efficiency such as algorithmic scalability, in the range of milliseconds, and synthesis runtime, in a hundred seconds, confirm that the program maintains a good performance as workloads grow without significant slowdowns. Besides, according to the results of the many different tests applied, SAFIMAM has proved to be competitive when compared to some other synthesis tools reported in the literature. Two design examples synthesized with SAFIMAM were implemented: a Pascal filter optimized in the stopband for Electromyogram (EMG) signals, implemented with AN231E04 Field Programmable Analog Arrays (FPAAs) embedded in the Anadigm QuadApex Development Board; and a Chebyshev Substrate Integrated Waveguide (SIW) filter for the fifth generation of wireless cellular technology (5G). Experimental and synthesis results agreement demonstrate the SAFIMAM reliability. In addition, when compared to some other EMG and 5G filters reported elsewhere, it is evident that the performance of the synthesized filter structures produced by the proposed software are also feasible.**

Link to graphical and video abstracts, and to code:
https://latamt.ieeer9.org/index.php/transactions/article/view/10184

***Index Terms*—Analog-Filters-Synthesis, GUI, MATLAB App Designer, Pascal-Filters, SAFIMAM.**

I. Introduction

THERE are a few systematic methods widely employed for the synthesis of analog filters, like those based on determining the corresponding transfer function, *H(s)*, by means of a well known approach such as the signal flow graphs [1], or the passive ladder *LC* filter simulation, which is also a common practice for the design of active filters. As part of the ladder *LC* simulation, the use of diverse approximation methods is involved. These methods allow the generation of *H(s)* such that it meets important requirements established by the prescribed form, either in magnitude, $|H(j\omega)|$, or phase, $\angle H(j\omega)$, of the frequency response of the filter [2]. Among the approximation methods that have been most studied, analysed, and used for decades are [3]: (1) the Butterworth approach, proposed by Stephen Butterworth and whose $|H(j\omega)|$ exhibits a maximally flat response in the bandpass; (2) the Chebyshev approaches, one with a $|H(j\omega)|$ response with ripple in the bandpass (type 1) and the other with a $|H(j\omega)|$ with ripple in the stopband (type 2), proposed by Pafnuty Lvovich Chebyshev; and (3) the elliptic approximation, whose $|H(j\omega)|$ response presents ripple in both bandpass and stopband, based on the work of Wilhelm Cauer.

Even though the aforementioned are broadly well known procedures, these are not the only available proposals. According to the literature, the Bessel–Thomson, with maximally flat group delay, and the Gaussian (Gaussian-shaped magnitude filter with excellent transient response) filter approximations also appear most frequently [4], followed closely by Legendre (also called Papoulis) [5], a monotonic passband with steeper rolloff than Butterworth, and Ultraspherical filters [6], with tunable parameter related to the order of the Gegenbauer polynomial. Finally, as an alternative to the Thomson for phase-optimized design, there are, at least, two options: the Bernstein approximation [7], whose key property lies in its linear phase with tunable parameters, and the Gammatone approximation [8], whose filter realizations possess an impulse response based on Gamma distribution modulated by a tone and exhibit asymmetric band-pass characteristics tuned by order and parameters.

Yet, in recent synthesis techniques with interesting attributes such as non-equiripple magnitude are available. The Pascal approximation, originally proposed by [9], Pascal filters exhibits a passband monotonic transition and stopband behavior similar, and even better in some cases, to the responses

The associate editor coordinating the review of this manuscript and approving it for publication was Adriana Vargas Martínez (*Corresponding author: Victor Hugo Hernández Juárez*).

Victor Hugo Hernández Juárez, L. A. Sánchez-Gaspariano, R. Torrealba-Meléndez, J. M. Muñoz-Pacheco, and L. D. C. Gómez-Pavón are with the Benemérita Universidad Autónoma de Puebla. Facultad de Ciencias de la Electrónica, Av. San Claudio y 18 Sur Edif. FCE1, Col. San Manuel, Ciudad Universitaria, Puebla, México (e-mails: hj224570062@alm.buap.mx, luis.sanchezgas@correo.buap.mx, richard.torrealba@correo.buap.mx, jesusm.pacheco@correo.buap.mx, and luz.gomez@correo.buap.mx).

C. Sánchez-López is with the Departamento de Electrónica, Universidad Autónoma de Tlaxcala, Calzada Apizaquito S/N, km 1.5, Apizaco, Tlaxcala, México (e-mail: csanchezl@uatx.mx).

C. Muñiz-Montero is with the Universidad Politécnica de Puebla, Ingeniería en Electrónica y Telecomunicaciones, Tercer Carril del Ejido, Serrano S/N, Juan C. Bonilla, Puebla, México (e-mail: carlos.muniz@uppuebla.edu.mx).

TABLE I
DETAILED BREAKDOWN OF THE FILTER DESIGN TOOLS AVAILABLE

Category	Tool	Approximations
Web-Plataform	LC Filter Design Tool [11]	*Butterworth, Chebyshev I Elliptic, Chebyshev II Bessel and Legendre*
	Webench [12]	*Butterworth, Chebyshev Bessel, Gaussian and Linear-Phase*
	Analog Filter Wizard [13]	*Butterworth, Chebyshev Bessel(via intuitive slider)*
	Online CADCOM [14]	*Does not perform design, Recommends external tools like FilterLab*
Manufacturer Solutions	FilterLab (Microchip) [15]	*Butterworth, Chebyshev Bessel*
	FilterCAD (Analog Devices) [16]	*Butterworth, Chebyshev Elliptic, Bessel and Minimum Q Elliptic*
	FilterPro (TI) [17]	*Butterworth, Chebyshev Bessel, Gaussian and Linear-Phase*
	Filter Wiz Lite [18]	*Butterworth, Chebyshev I Chebyshev II, Elliptic and Bessel*
	CoilcraftLCTool [19]	*Exclusively Elliptic*
	RFHammer [20]	*Chebyshev and Bessel*
Software Specific	FILTER_GUI [21]	*Butterworth and Chebyshev*
	MWFilterDesign [22]	*Exclusively Butterworth*
	FILTERD (Mathcad) [23]	*Butterworth, Chebyshev and Cauer(Low-pass only)*
	Elsie [24]	*Butterworth, Chebyshev Elliptic, Bessel, Gaussian Constant-K and M-derived*

generated by the Chebyshev filters since relatively low filter orders are obtained, with the possibility of reducing the ripple in the bandpass [10]. Thus, Pascal filters present an intermediate performance between Butterworth (maximally flat) and Chebyshev (equiripple). However, neither synthesis nor simulation tools for Pascal filters are at disposal. There is an important amount of analog filter design tools, mainly Specific software-based (MATLAB) interfaces, web platforms, and manufacturer-solutions. Table I summarizes their main features. The key aspects of these tools are: the LC Filter Design Tool (Web) and Elsie (Desktop) offer the widest variety of classical and specialized approximations, including rarer types like Legendre or M-derived filters; on the other hand, most manufacturer tools (TI, Microchip, Analog Devices) focus on the "Big Three" (Butterworth, Chebyshev, and Bessel) because they are the most common for active op-amp implementations; further, tools supporting Elliptic (Cauer) approximations, such as the Coilcraft tool or FilterCAD, are ideal when a very sharp transition between the passband and stopband is required; additionally, If your design requirements involve constant group delay, tools supporting Bessel or Gaussian responses are available across all three categories.

This work presents a *Graphical User Interface* (*GUI*),

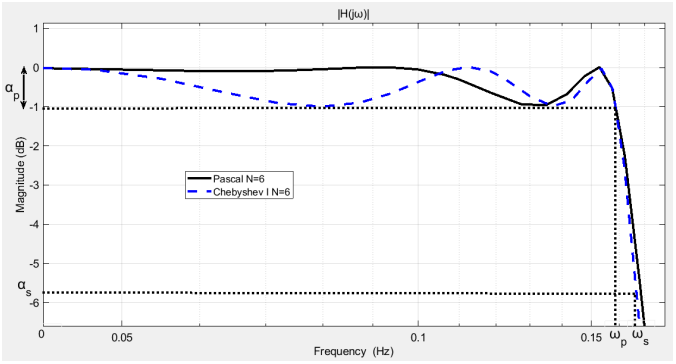

Fig. 1. $|H(j\omega)|$ Pascal response of a 6th order filter vs the corresponding 6th order Chebyshev equiripple response [25].

named SAFIMAM (acronym of Synthesis of Analog Filters in MATLAB by Approximation Methods), developed in MATLAB App Designer capable of carrying out the synthesis of analog filters based on approximation methods, including the Pascal approach, which is the main contribution of this work, at top and intermediate levels, starting from three design specifications: the bandpass ripple, the attenuation in the stopband, and the transition ratio between the stopband and the bandpass (ω_s/ω_p). Depending on the needs of the user, the program delivers: (1) the order, (2) the transfer function, (3) the frequency response, (4) the frequency transformation, (5) the π or T *LC* ladder structure of the filter, and (6) the impedance transformation of the *LC* ladder.

The paper is organized as follows: in section 2, the Pascal approximation method for normalized-lowpass filter synthesis is described; moreover, the description of the proposed software architecture and its functionalities are discussed; later, on section 3 some representative examples are presented, specifically an active Pascal filter optimized in the stopband for Electromyogram (EMG) signals, implemented with AN231E04 Field Programmable Analog Arrays (FPAAs) embedded in the Anadigm QuadApex Development Board. Additionally, a Chebyshev Substrate Integrated Waveguide (SIW) filter for the fifth generation of wireless cellular technology (5G) is reported; the discussion about the attained results can be found in section 4; finally, the conclusions are drawn in Section 5.

II. SYNTHESIS-BASED ANALOG ELECTRONIC FILTERS IN MATLAB BY APPROXIMATION METHODS

There are already functions in MATLAB for the computation of parameters such as the order, the transfer function and some frequency transformations of analog filters through classical approximation methods. Now, with the development of the proposed set of functions for the synthesis of analog filters by means of the Pascal approximation method, there is the chance of building up a comprehensive tool capable of synthesizing analog filter structures with either classical or Pascal approximation mechanisms. The benefits of such program in terms of design solutions are promising: simplified calculation without determinants, systematic design and efficiency, flexible filter characteristics, improved handling of passive components and reduced design time, among others.

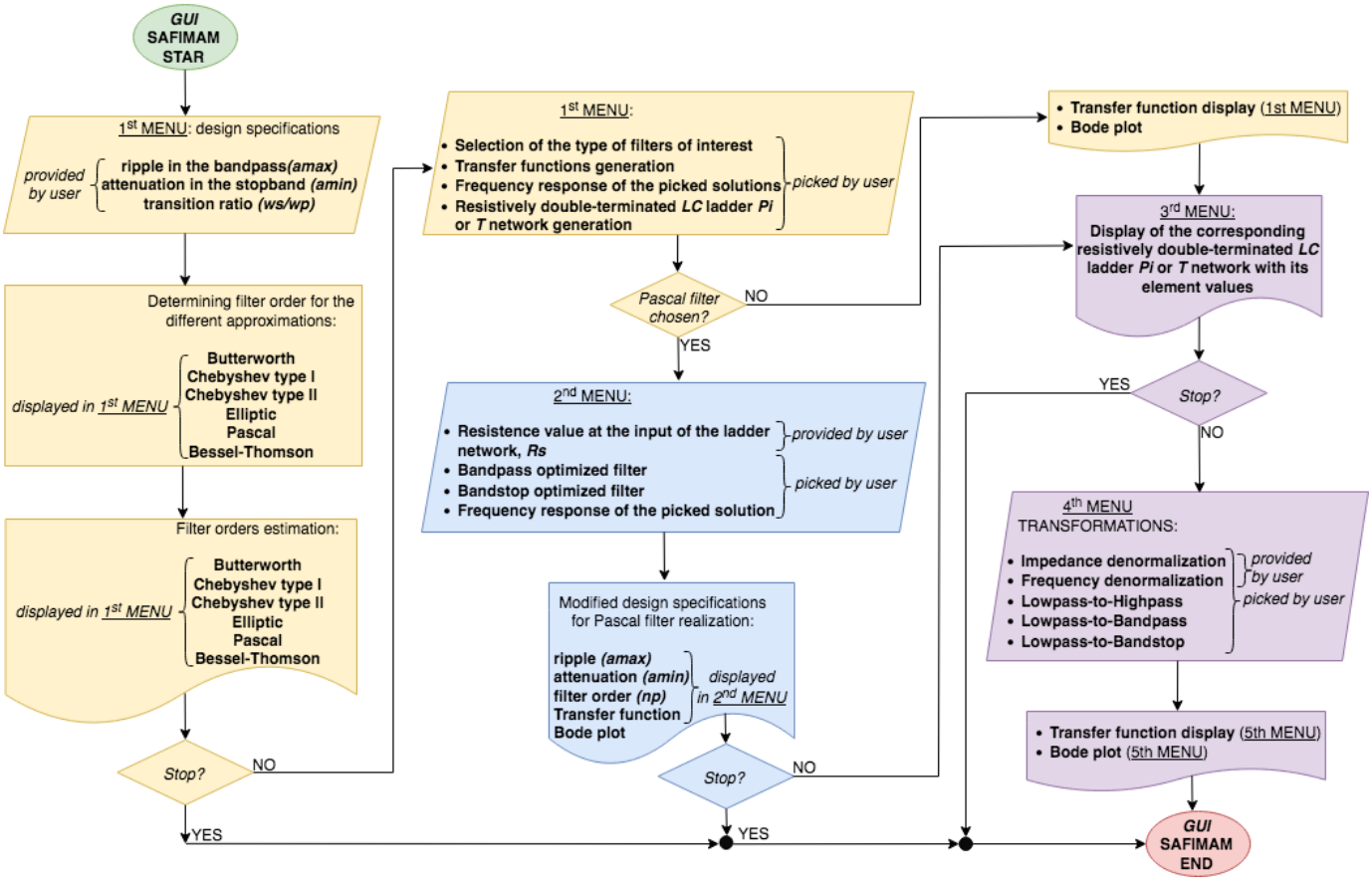

Fig. 2. Operational flowchart of the developed GUI, SAFIMAM. The pipeline guides the user from initial design specifications (a_{max}, a_{min}, ω_s/ω_p) through filter order estimation for classical and Pascal approximations. It also details the execution paths for synthesizing resistively double-terminated LC ladder networks (Π or T topologies), and a comprehensive engine for frequency/impedance transformations and denormalization.

A (*GUI*) called SAFIMAM, developed in MATLAB App Designer, is proposed. Even though SAFIMAM operates exclusively in MATLAB, a student version is enough for its execution without loss of functionality.

A. The normalized Pascal Lowpass Filter

In many signal processing applications, special attention is paid to the magnitude function of $H(s)$ even though any modification on this will also have an implication on the phase function. This is the case of normalized lowpass filters, whose relevance is notorious since these are the basis for the synthesis of more complex filters [2]. The normalized transfer function of any lowpass filter is that of the form [3]:

$$|H(j\omega)|^2 = \frac{1}{1+F(\omega^2)} \tag{1}$$

Depending on the nature of the polynomial $F(\omega^2)$, there will be a given behavior of the frequency response of the filter. In the normalized Pascal lowpass filter, $F(\omega^2)$ takes the form of the modified Pascal polynomial of n-th order, i.e. $F(\omega^2) = \lambda^2 P_D^2(N,\omega)$, where $P_D(N,\omega)$ is the Pascal polynomial of n-th order, and λ is a constant computed according to the specifications from the bandstop (ω_s), as well as the bandpass ripple and the bandstop attenuation (A_{max} and A_{min}, respectively) [10]. It is important to mention that the λ factor cannot take any value, it is bounded within the neighborhood $\lambda_{min} < \lambda < \lambda_{max}$, and it turns out that [9]

$$\lambda_{min} = \frac{\sqrt{10^{Amin/10}-1}}{|P_D(N,\omega_s)|}, \qquad \lambda_{max} = \frac{\sqrt{10^{Amax/10}-1}}{|P_D(N,1)|}, \tag{2}$$

The convenience of using λ_{max} or λ_{min} depends on the design needs. If a low order filter is required, then λ_{max} is more advantageous since it produces a bandstop optimized response, which typically comes from a low order filter. On the other hand, if a low ripple in the bandpass is demanded, then a bandpass optimized filter is convenient, which are obtained when λ_{min} is chosen. Contrary to the classical approximation methods, the synthesis of a transfer function through the Pascal approach is sensitive to filter order parity conditions [9], [10]. Furthermore, if the aim of the synthesis is to reach a resistively double-terminated LC ladder network, further considerations regarding the matching between termination resistors, R_S and R_L, must be considered [9], [10]. Thus, synthesis of analog filters by means of the Pascal approximation is more cumbersome. Yet, due to its interesting attribute of non-equiripple magnitude, the Pascal approximation remains appealing inasmuch as it exhibits a performance similar to the

responses generated by the Chebyshev filters with relatively low order filter, but with the profit of a reduced ripple in the bandpass [10]. In order to appreciate this, Fig. 1 illustrates the frequency response of a sixth order Pascal filter and its Chebyshev counterpart [25].

B. Software Architecture and Functionalities

The proposed Graphical User Interface (GUI) for analog filter synthesis is structured into five main menus, as illustrated in Fig. 2. The architecture is designed to support a top-down synthesis workflow for classical approximation methods as well as the Pascal approach, based on user-defined design specifications: passband ripple (α_{max} or A_{max}), stopband attenuation (α_{min} or A_{min}), transition ratio (ω_s/ω_p), and input resistance (R_s).

- **Menu 1 (Design Specifications & Classical Approximations):** Collects the initial design parameters (A_{min}, A_{max}, and ω_s/ω_p), computes and displays the minimum filter order, and allows the user to select the approximation type. It handles transfer function generation, Bode plot rendering, and the selection of the corresponding *LC* ladder network topology.
- **Menu 2 (Pascal Filter Configuration):** Activated exclusively for the Pascal approximation. It accepts the input resistance R_s and the optimization type (bandpass or bandstop optimized). Upon execution, it displays the recalculated ripple, attenuation, filter order, and transfer function, while also providing independent Bode plot generation.
- **Menu 3 (Network Realization):** Displays the synthesized, resistively double-terminated *LC* ladder network in either a T or π configuration, populated with calculated component values.
- **Menu 4 (Frequency and Impedance Transformations):** Executes frequency and impedance denormalizations, mapping the prototype lowpass filter to highpass, bandpass, or bandreject configurations.
- **Menu 5 (Transformed Filter Analysis):** Renders the final transfer function and Bode plot of the transformed, denormalized filter.

The first four menus are shown in Fig. 3, while the fifth menu is demonstrated via an application example in Section 3. The complete, open-source SAFIMAM package—including the GUI source code, licensing, and synthesis examples—is available in the GitHub repository: https://github.com/VICTORHUGOHJ/SAFIMAM.

The proposed *GUI* allows the user to calculate at different levels, from top to down, the results concerned to the synthesis of analog filters through any classical approximation method, and also the Pascal approach. Some of the results that can be computed by the *GUI* involves:

1) *The filter order.*
2) *The selection of the type of approximation method for the synthesis of the filter.*
3) *The transfer function generation.*
4) *The Bode plot.*
5) *The impedance and frequency denormalizations.*
6) *The lowpass filter transformation to highpass, bandpass and bandreject filters.*
7) *The selection of either of the Pascal filters available, the passband optimized and the stopband optimized.*
8) *The resistively double terminated LC ladder network, in π or T type, of any of the approximations methods employed for the synthesis.*

All these results can be obtained by providing a few design specifications to the *GUI*: (1) the ripple in the bandpass, α_{max}, (2) the attenuation in the bandstop, α_{min}, (3) the transition ratio, (ω_s/ω_p), and (4) the resistance value at the input of the *LC* ladder network, R_s.

C. Performance Metrics

Prior to the demonstrative examples, we analyze the GUI's computational efficiency, algorithmic scalability, and synthesis runtime. The scalability of the integrated approximation methods was assessed via the following simulation protocol:

- **Order Determination:** Design specifications — including passband ripple (A_{max}), stopband attenuation (A_{min}), and selectivity (ω_s/ω_p)— were evaluated to generate filter orders $n \in [2, 21]$. SAFIMAM current upper limit of order 21 is fundamentally bound by the availability of Pascal polynomial coefficients. While literature traditionally tabulates these characteristics only up to order 15 [26], we successfully extended the polynomial generation to order 21 using the iterative technique from [10]. While mathematically feasible to scale beyond order 21, we deliberately capped the synthesis engine here to maintain strict comparative uniformity with the other approximation methods integrated into the platform.
- **Synthesis and Transfer Functions:** For each approximation method, the corresponding transfer functions were derived, followed by the synthesis of element values for both T and π network topologies.
- **Parametric Transformations:** Systematic frequency (HPF, BPF, BSF) and impedance transformations were executed. This involved a multidimensional test matrix comprising 10 discrete impedance values, 10 frequency points, and 10 bandwidth ranges.
- **Network Scaling:** A secondary impedance transformation was applied to all frequency-transformed networks. This final stage yielded scaled element values across the full range of orders and approximation methods, ensuring a comprehensive validation of the synthesis engine.

The evaluation protocol was extended to include the synthesis of ideal Pascal filters. In this specialized simulation case, the transfer function is derived by disregarding the typical constraints inherent in even-order Pascal implementations. Key characteristics of this synthesis include: impedance independence, transfer functions are calculated without restricted internal or network resistance values, which conventionally modulate filter gain; normalized gain, the numerator polynomial assumes a normalized gain (1Ω), while the denominator is defined strictly by the coefficients of the Pascal polynomial; and direct response observation, this specific GUI module focuses exclusively on the ideal frequency response, bypassing

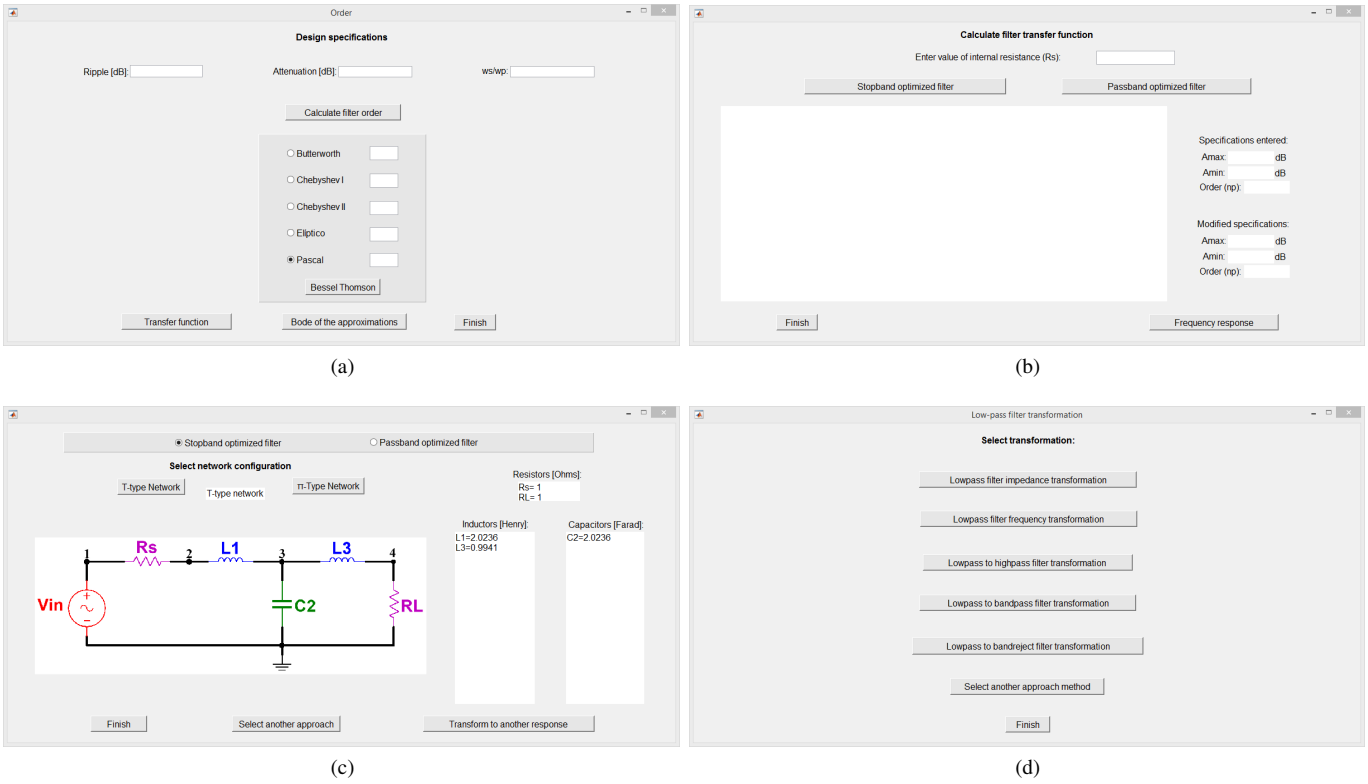

Fig. 3. The four MENUs displayed by the developed GUI, SAFIMAM: (a) Menu for design specification entry and filter order estimation across multiple approximations; (b) Menu dedicated to Pascal filter optimization and specification modification; (c) Menu displaying the synthesized resistively double-terminated LC ladder network topology along with computed component values; (d) Menu providing options for impedance/frequency denormalization and frequency band transformations.

subsequent parametric transformations and electrical network synthesis.

The Bessel-Thomson synthesis was evaluated using a delay-centric characterization protocol, distinct from magnitude-based methods. The procedure systematically sweeps delay specifications to generate multiple filter orders, followed by a four-tiered transfer function derivation:

- **Normalization and Scaling.** Transfer functions are generated for: (1) Normalized group delay ($\tau = 1s$); (2) Normalized cutoff frequency ($\omega_c = 1rad/s$); (3) Variable cutoff frequencies ($f_c \in [100, 105]Hz$); (4) Specific group delay targets ($\tau \in [6.61, 17.9]\mu s$).
- **Network Realization.** Low-pass RLC element values are synthesized for both T and π topologies across all calculated functions.
- **Impedance Scaling.** A final frequency transformation is executed by scaling the synthesized network parameters across a discrete impedance vector $Z \in [10, 1000]\Omega$.

Fig. 4 summarizes the scalability results for each approximation method. It can be appreciated that in all the cases, as the filter order rises it also does the computing time, more or less proportionally with exception of the Elliptic and Bessel Thomson approaches. The first showing a more stepped computing time from filter order of 15 till 21, and the second showing an abrupt rise of the computing time from filter order of 10 to 11. In any case, the computing time increase is within the milliseconds range, which is good enough for practically any user.

The computational overhead for the magnitude-based approximation methods was quantified using a procedure analogous to the scalability assessment, refined for temporal isolation. Specifically, a single design specification (A_{max}, A_{min}, and ω_s/ω_p) was applied per method to yield unique filter orders. The synthesis latency—defined as the interval from specification input to the determination of final transformed element values—was recorded for all parametric transformations across the previously defined impedance, frequency, and bandwidth vectors.

For the *Bessel-Thomson* methods, runtime was characterized by evaluating a range of group delays to generate multiple orders. The performance metrics reflect the duration required to compute the four transfer function variants and execute the subsequent impedance scaling of the network parameters. The cumulative execution times, representing the total synthesis duration across all approximation methods and design stages, are consolidated in Table II. As can be seen, the largest computational overhead lies on the Pascal approach. This is mainly due to its design constraints, i.e. generally, odd-order filters do not have restrictions on the maximum allowable passband ripple (A_{max}) when designing passive filters whereas even-order filters may encounter a "*design issue*" where direct synthesis is restricted. This occurs when the required passive termination resistance (R_S, R_L) makes the passband ripple

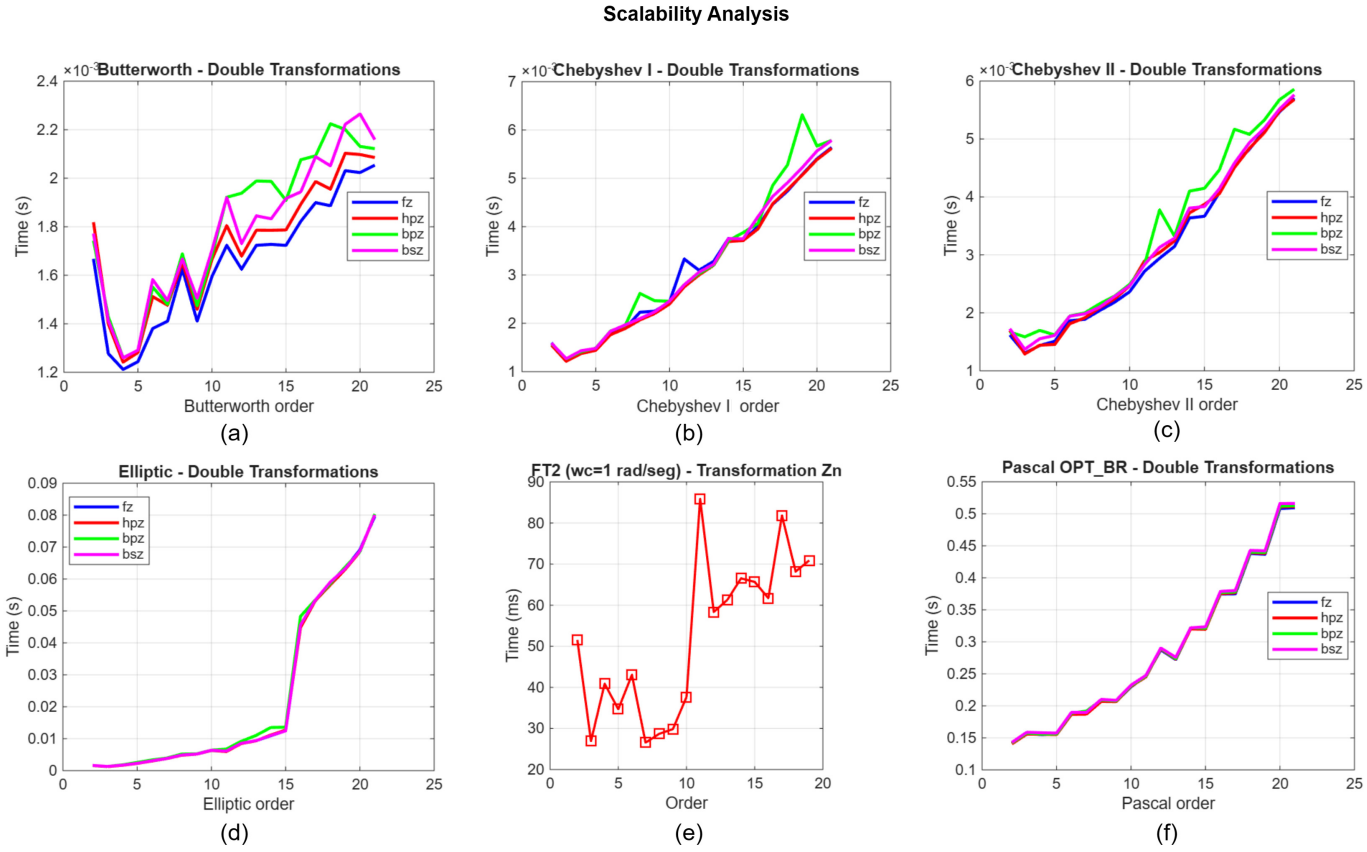

Fig. 4. Scalability and execution time analysis of SAFIMAM across various filter approximations for orders 2 to 21, evaluating four transformation types (fz, hpz, bpz, bsz): (a) Butterworh; (b) Chebyshev type I; (c) Chebyshev type II; (d) Elliptic; (e) Bessel Thomson; (f) and Pascal.

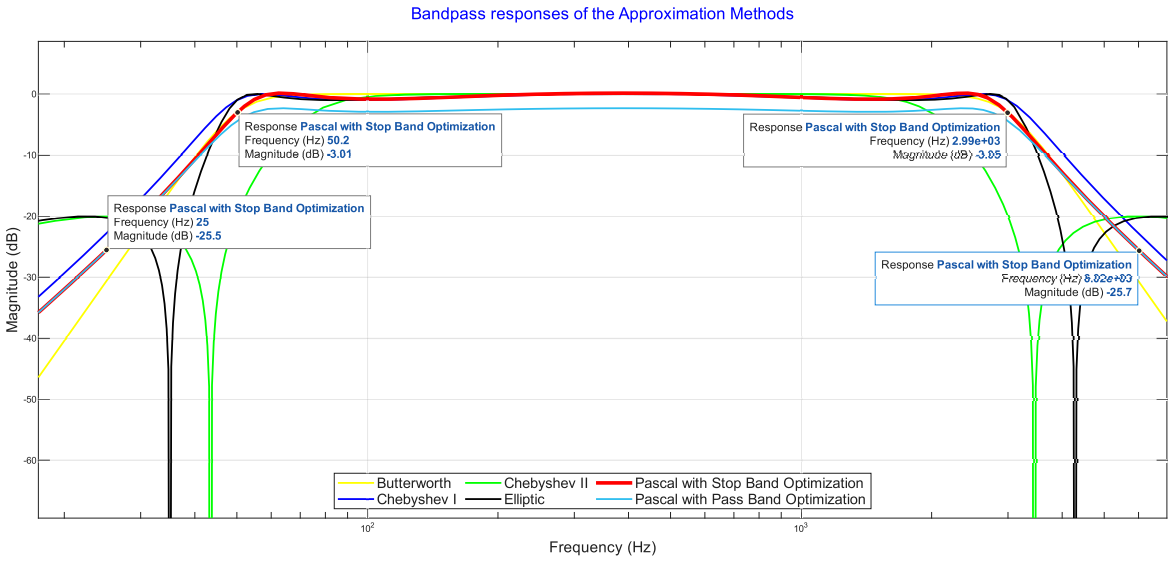

Fig. 5. Frequency responses of the bandpass filters for EMG signals synthesized by SAFIMAM.

too high, specifically when $A_{max} > A_0$, where A_0 is the attenuation at DC. However, the whole synthesis process, once having the input parameters till delivering a T or π double resistor terminated ladder whose frequency response fulfills the design requirements given by the user with the option to select have up to six different approximation methods, including the Pascal approach, is done in less than two minutes. This is a very convenient time if we take into account that the tool synthesizes the whole filter based solely on 3 specifications.

TABLE II
RUNTIME OF SAFIMAM FOR CLASSIC METHODS, PASCAL APPROACH, BESSEL-THOMSON METHOD AND TOTAL

	Classic approaches	Pascal approach	Bessel-Thomson approach	Total Runtime
Runtime	$3.13s$	$100.86s$	$1.78s$	$105.78s$

III. REPRESENTATIVE EXAMPLES

In order to validate the results of the proposed *GUI*, SAFIMAM, the filter synthesis for two different technologies, with both simulation and experimental results, are presented: the first is an active bandpass Pascal Filter with optimized stopband, for *EMG* signals; and the second is a bandpass Chebyshev type I filter for 5G technology applications. The Pascal filter was assembled with AN231E04 FPAAs embedded in the Anadigm QuadApex Development Board while the Chebyshev filter was transformed for its realization with waveguides.

A. Bandpass Pascal Filter for EMG Signals

EMG encompasses the analysis of electrical activity generated in nerves and muscles through the use of electrodes. The measurements from *EMG* provide valuable information about physiology and muscle activation patterns. In addition, it can be used in the diagnosis of pathologies affecting the peripheral nervous system, functional alterations of the nerve roots, as well as muscle and neuromuscular junction pathologies. The range of frequencies covered by these signals range from 50Hz to 3KHz as indicated in [27]. Typically, prefiltering is used in this kind of technologies. A bandpass pre-filter with an attenuation of 20dB and a maximum ripple in the bandpass of 1dB is adopted [28]. Thus, taking into account these specifications and a transition ratio (ω_s/ω_p) of 2, SAFIMAM yields the results summarized in Table III and depicted in Fig. 5. According to these, Chebyshev type 1, Elliptic and Pascal optimized in the stopband produce similar responses with a third order filter structure. Before prototyping, Monte Carlo tolerance simulation for the active Pascal filter of Fig. 7 was carried out in order to verify its robustness. Fig. 6 illustrates the Monte Carlo analysis (over 100 runs) for the case of the attenuation of the frequency response at cutoff (f_1 and f_2) and center frequencies (f_0). A reference level of -6dB was employed since 50Ω load and source resistors were used. The median for attenuation at f_1 was of -2.89dB with a standard deviation (σ) of 0.25dB whereas the median (μ) at f_2 was -3.84dB with a σ of 0.27dB. Finally, the μ for attenuation at f_0 was -0.95dB with a of 0.13dB. These results demonstrate the feasibility of the proposed EMG active filter.

The implementation of this circuit was done as follows: first, from the Pascal bandpass transfer function (*BPTF*) with optimization in the stopband in Table III, a π type ladder network is picked; once the network is provided by SAFIMAM, with its corresponding frequency and impedance transformation, we proceed to perform the active simulation of the passive ladder via a direct simulation method, where coils are replaced by Generalized Impedance Converter (GIC) inductors; finally, the active architecture is accomplished by means of AN231E04 FPAAs embedded in the Anadigm QuadApex Development Board. Subsequently, the active filter was tested in the multifunction instrument *Digilent Analog Discovery 2*, taking advantage of its Bode analyzer. Fig. 7 depicts the schematic, the test-setup and the experimental frequency response of active Pascal filter optimized in the stopband. On the other hand, Table IV shows simulation results of the synthesized filter along with experimental results of its corresponding active realization.

As expected, the design specifications provided to SAFIMAM, which in turn are the triggers for the synthesis process carried out by the *GUI*, match with both, the simulation results of the *GUI* and the experimental results. Considering that the expected center frequency is 1525Hz, and that simulation result is 1520Hz, a relative error of $\approx 0.3\%$ for this case is exhibited by the *GUI* meanwhile the experimental center frequency has a 2.33% error. The expected bandwidth is 2950Hz, thus with a value of 2939.5Hz, the simulation results presents an error of $\approx 0.3\%$ whereas the experimental error, with a result of 2878.64Hz, is of $\approx 2.4\%$. Cutoff frequencies errors for simulation are of $\approx 1\%$ and $\approx 0.3\%$, respectively, and Cutoff frequency errors of the prototype are $\approx 0.2\%$ and $\approx 2.4\%$, respectively. The errors for the attenuation in the bandpass are of $\approx 2\%$ for the simulation and $\approx 0.2\%$ for the prototype. The ripple in the bandpass error of the *GUI* is $\approx 3\%$ and the error of the prototype is 0%. Finally, the error for the attenuation in the bandstop at the specified (ω_s/ω_p) ratio is of $\approx 0.4\%$ for the *GUI* and $\approx 1.6\%$ for the prototype.

Errors produced by SAFIMAM are inherent to the nature of the approximation method employed: Butterworth, Chebyshev I, Chebyshev II, Elliptic, Bessel-Thomson or Pascal. In fact, these are called approximation methods because they approximate the synthesized response to the specified value. On the other hand, errors exhibited by the prototype are of both random and systematic type. Diverse factors such as tolerance of the circuit elements and the precision of the test equipment affect. Finally, since biomedical filtering involves noise-sensitive signals, additional evaluation of noise floor analysis would be of interest. For this purpose, Fig. 8 shows the experimental setup for the measurement of the noise floor of the FPAA EMG Pascal filter. The active circuit was biased and no input signal was provided; thus, the output noise generated at the output port was of approximately $1.69mV_{rms}$, an acceptable value for EMG signal processing if we consider that EMG signals achieved up to $5mV$ voltage swing.

B. Bandpass Filter for 5G Technology

5G technology demands a considerable amount of new and harmonized mobile spectrum frequency ranges in order to provide wide network coverage. The bands of interest are below 1GHz, between 1 and 6 GHz (but not restricted to), and above 6GHz [29]. In this design example, we focus on the portion of the spectrum between 3.4GHz and the 3.79GHz, for planar microstrip patch antennas for 5G wireless applications.

Design specifications, taken from the spectral mask in [30], for a Chebyshev type I filter are: a maximum ripple in the

TABLE III
SUMMARY OF SOME RESULTS PRODUCED BY SAFIMAM FOR THE SYNTHESIS OF THE FILTER FOR EMG SIGNALS. *LPTF* AND *BPTF* ARE LOWPASS AND BANDPASS TRANSFER FUNCTIONS, RESPECTIVELY

Chebyshev Approximation Method I, Order 3	
LPTF	$\frac{0.4913}{s^3+0.9883s^2+1.238s+0.4913}$
BPTF	$\frac{3.129\times10^{12}s^3}{s^6+1.832\times10^4s^5+4.432\times10^8s^4+3.346\times10^{12}s^3+2.625\times10^{15}s^2+6.424\times10^{17}s+2.077\times10^{20}}$
π Type network	$R_s=100\Omega$, $R_L=100\Omega$, $L_1=0.15468H$, $C_1=1.0917\times10^{-6}F$, $L_2=0.0053633H$, $C_2=3.1486\times10^{-5}F$, $L_3=0.15468H$, $C_3=1.0917\times10^{-6}F$
Elliptic Approximation Method, Order 3	
LPTF	$\frac{0.3206s^2+0.6647}{s^3+0.9666s^2+1.241s+0.6647}$
BPTF	$\frac{5942s^5+4.303\times10^{12}s^3+2.084\times10^{17}s}{s^6+1.792\times10^4s^5+4.44\times10^8s^4+4.445\times10^{12}s^3+2.629\times10^{15}s^2+6.283\times10^{17}s+2.077\times10^{20}}$
π Type network	$R_s=100\Omega$, $R_L=100\Omega$, $L_{1p}=0.20144H$, $C_1=8.383\times10^{-7}F$, $L_{2p}=0.40592H$, $C_2=4.1602\times10^{-7}F$, $L_2=0.0033745H$, $C_{2s}=5.0042\times10^{-5}F$ $L_{3p}=0.20144H$, $C_3=8.383\times10^{-7}F$
Pascal Approximation Method with Optimization in the Stopband, Order 3	
LPTF	$\frac{0.5}{s^3+0.9883s^2+1.238s+0.4913}$
BPTF	$\frac{2.374\times10^{12}s^3}{s^6+1.661\times10^4s^5+3.676\times10^8s^4+2.53\times10^{12}s^3+2.179\times10^{15}s^2+5.837\times10^{17}s+2.083\times10^{20}}$
πType network	$R_s=100\Omega$, $R_L=100\Omega$, $L_1=0.14012H$, $C_1=1.204\times10^{-6}F$, $L_2=0.0059146H$, $C_2=2.8523\times10^{-5}F$, $L_3=0.14012H$, $C_3=1.204\times10^{-6}F$

TABLE IV
SIMULATION VS EXPERIMENTAL RESULTS OF THE SYNTHESIZED EMG IN SAFIMAM

Parameters	SAFIMAM	Experimental
Center frequency	1520 Hz	1489.37 Hz
Bandwidth	2939.5 Hz	2878.64 Hz
Cutoff frequency 1	50.5 Hz	50.11 Hz
Cutoff frequency 2	2990 Hz	2928.64 Hz
Attenuation in the bandpass	5.88 dB	5.99 dB
Ripple in the bandpass	0.97dB	1dB
Attenuation in the bandstop	19.92dB	20.31dB

bandpass of 1dB, a minimum attenuation in the bandstop of 25dB and a transition ratio of 2.5. After providing this information to SAFIMAM along with the required bandwidth and center frequency, the bandpass *LC* T network exhibited in Fig. 9 is reached. Hereafter, impedance transformation such that $R_S = R_L = 50\Omega$ is performed; finally, for high frequency implementation, Richard's transformation is realized yielding in the Substrate Integrated Waveguide (SIW) shown at the top of Fig. 10. The size of the designed SIW is $116.71mm \times 31.79mm$. The implementation of the SIW was carried out in a PC board with a Rogers 4003C substrate, whose loss tangent is $\delta = 0.0023$, its relative permittivity $\varepsilon_r = 3.55$ and with a thickness of $h = 1.524mm$. An ANRITSU Vector Network Analyzer model MS4644B was used. The experimental results depicted in Fig. 10 include the S_{11} and S_{12} parameters. The cutoff frequencies, the center frequency and the ripple in the pass band and attenuation in the stopband are pointed out. Since the implemented SIW filter corresponds to a passive ladder filter, then the S_{12} parameter equals the S_{21} (forward transmission) parameter. Thus, along with the shape of the S_{11} parameter in the pass band, in this case the S_{12} parameter indicates a good match in the band of interest. According to the results in Fig. 10, the quality factor of this filter (Q), given by the ratio between the center frequency and the bandwidth, is of 9.47. This Q value indicates that the filter has moderate selectivity, meaning that it allows

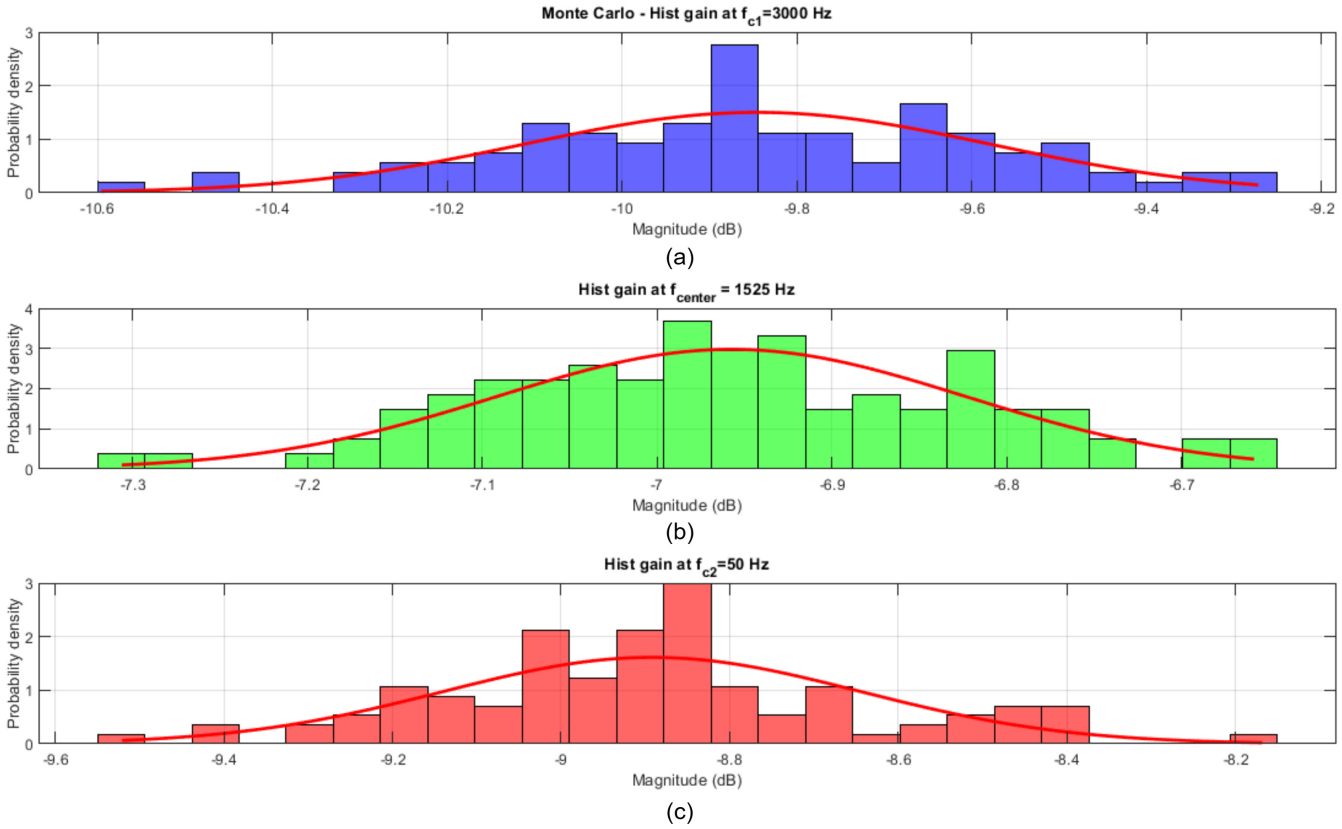

Fig. 6. Monte Carlo simulation of frequency response of the magnitude of the Pascal filter for EMG: (a) histogram of the upper cutoff frequency, $f_{c1} = 3000$ Hz; (b) histogram of the center frequency, $f_{center} = 1525$ Hz; histogram of the lower cutoff frequency, $f_{c2} = 50$ Hz.

signals to pass through the passband with minimal losses while effectively attenuating signals outside this band.

Furthermore, the Voltage Standing Wave Ratio (VSWR) parameter, a dimensionless parameter that indicates the degree of impedance matching between the filter and the transmission line, can be calculated with the aid of parameter S_{11}. VSWR values close to 1 indicate a good match and a minimal reflections, while higher values beyond 1 indicate mismatch and increased reflection losses. Based on the measurements, a frequency range between 3.46 GHz and 3.76 GHz was identified where $VSWR < 2$. This range is highlighted in Fig. 10, where the plot shows the region where the filter exhibits good impedance matching, ensuring efficient and stable signal transfer within the band of interest. The extent of this range coincides with the expected passband of the filter, confirming that the measured performance is consistent with the design and the frequencies of interest.

Finally, Table V shows simulation results of the synthesized filter along with experimental results of its corresponding Waveguide realization. As can be seen, experimental and simulation results agree with design specifications. Considering that the expected center frequency is 3.595GHz, and that simulation result is 3.625Hz, a relative error of $\approx 0.8\%$ for this case is exhibited by the *GUI* meanwhile the experimental center frequency has a 0.14% error. The expected bandwidth is 390MHz, thus with a value of 370MHz, the simulation results presents an error of $\approx 5.1\%$ whereas the experimental error,

TABLE V
SIMULATION VS EXPERIMENTAL RESULTS OF THE SYNTHESIZED SIW FILTER IN SAFIMAM

Parameters	SAFIMAM	Experimental
Center frequency	3.625 GHz	3.6 GHz
Bandwidth	0.37 GHz	0.38 GHz
Cutoff frequency 1	3.44 GHz	3.44 GHz
Cutoff frequency 2	3.81 GHz	3.82 GHz
Attenuation in the bandpass	0 dB	-1.11 dB
Ripple in the bandpass	1 dB	0.91 dB
Attenuation in the bandstop	25 dB	25.006 dB

with a result of 380MHz, is of $\approx 2.6\%$. Cutoff frequency errors for simulation are of $\approx 1.2\%$ and $\approx 0.5\%$, respectively, and Cutoff frequency errors of the prototype are $\approx 2.6\%$ and $\approx 0.8\%$, respectively. The errors for the attenuation in the bandpass are of 0% for the simulation and $\approx 12\%$ for the prototype. The ripple in the bandpass error of the *GUI* is 0% and the error of the prototype is 9%. Finally, the error for the attenuation in the bandstop at the specified (ω_s/ω_p) ratio is of 0% for the *GUI* and $\approx 0.02\%$ for the prototype.

As in the previous case with the *EMG* filter, errors produced by SAFIMAM are inherent to the nature of the approximation method employed. In addition, since both simulation and experimental results reported herein correspond to the transformed ladder network into a SIW filter, then errors produced by the Richard's transformation are also added up. The

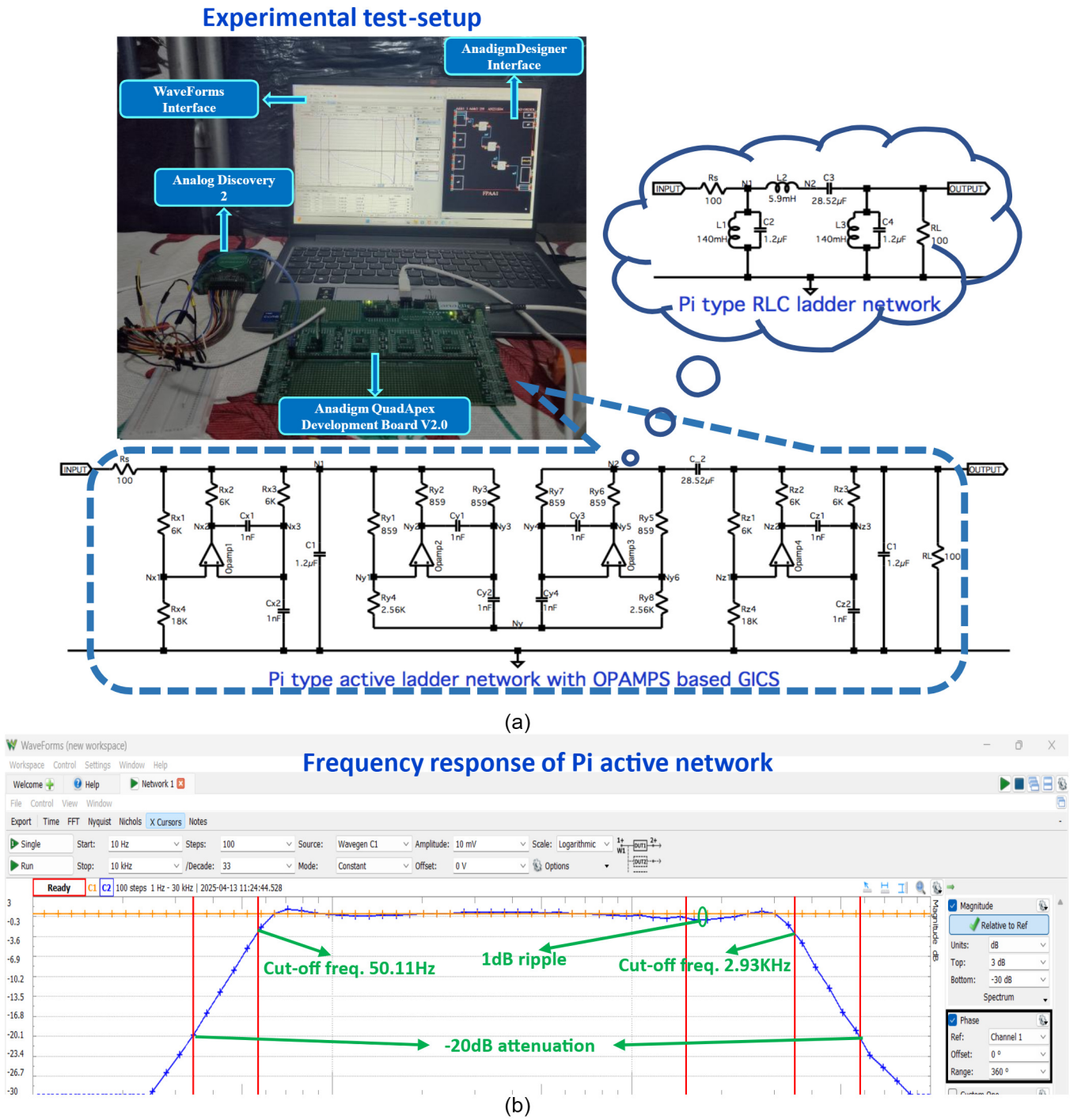

Fig. 7. Implementation of the 3rd order Pascal filter optimized in the stopband: (a) Experimental test-setup by means of an Anadigm Quad Apex Development FPAA Board and a Diligent Analog Discovery 2 measurement instrument; (b) experimental frequency response of the π type active ladder network.

reason because experimental results show a larger deviation compared to simulation results lies in: fabrication tolerances (PCB Process) via diameter and spacing, etching accuracy and misalignment; substrate material characteristics such as dielectric constant variation, loss tangent error, substrate thickness; transition and assembly issues like the transition from the SMA connector to the SIW structure or the variations in soldering quality, and also measurement setup errors, to name a few.

IV. Discussion

Filter synthesis translates mathematical abstractions into physical hardware. Thus, discrepancies invariably arise between ideal simulations and experimental results due to component non-idealities, structural parasitics, and environmental factors. These deviations are categorized into systematic and

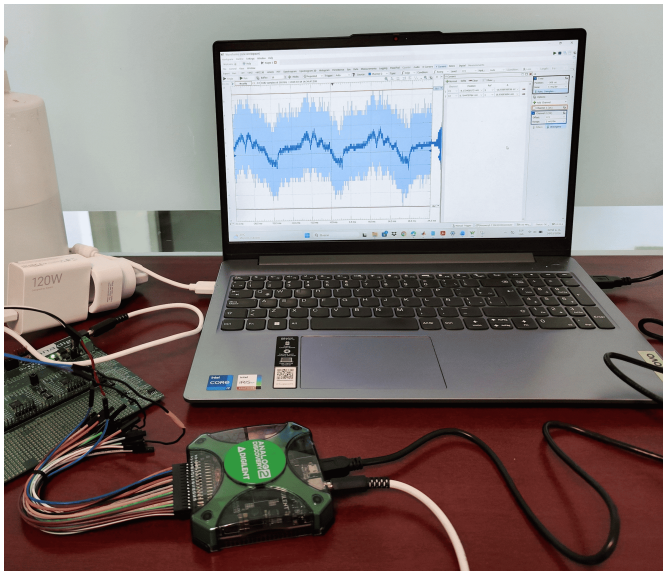

Fig. 8. Floor noise measurement of the active Pascal filter.

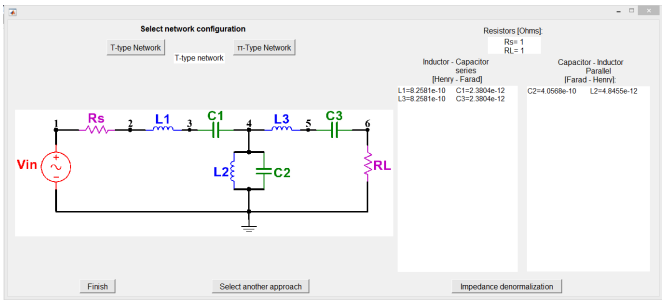

Fig. 9. Bandpass Chebyshev type I filter for 5G synthesized by SAFIMAM.

random error sources. Systematic errors are predictable, deterministic, and directionally biased deviations governed by consistent physical laws. Examples include finite active-device impedances, capacitor equivalent series resistance, inductor self-resonance, and PCB trace parasitics. Because they are reproducible, these errors can be accurately compensated for during the design phase. On the other hand, Random Errors are stochastic, unpredictable variations that fluctuate between individual units according to statistical distributions. These include manufacturing tolerances of passive components, localized PCB substrate variations, thermal noise, and environmental temperature coefficients. While unavoidable, their impact can be mitigated by incorporating robust design techniques. Thereby, the reason because the deviations between SAFIMAM and experimental results attained in both cases, bandpass Pascal filter for EMG and bandpass filter for 5G, are minimal is due to careful considerations in the design stage to avoid introducing systematic errors and minimize possible random errors.

To quantify the structural divergence between the simulated and experimental frequency responses without introducing interpolation errors from mismatched frequency sampling grids, a two-sample Kolmogorov-Smirnov test (KS-test) was utilized. Even though the KS-test quantifies the distance between

TABLE VI
COMPARISON AMONG DIFFERENT FILTER SYNTHESIS TOOLS INCLUDING SAFIMAM FOR THE SYNTHESIS OF A CHEBYSHEV TYPE I PASSBAND FILTER FOR EMG

Simulation Results	SAFIMAM	Filter D. Tool	Analog F. Wizard	LC Filter D. Tool	Filter Lab
$f_0[Hz]$	1520	1647.5	1525	1647.4	1678.35
% of error	0.32%	8.03%	0%	8.02%	10.05%
$BW[Hz]$	2939.5	3203	2950	3202.2	3265.3
% of error	0.35%	8.5%	0%	8.5%	10.6%
$f_1[Hz]$	50.5	46	50	48.55	45.7
% of error	1%	8%	0%	8.4%	8.6%
$f_2[Hz]$	2990	3249	3000	3249	3311
% of error	0.33%	8.3%	0%	8.3%	10.36%
$A_{max}[dB]$	0.97	1	1.02	1.003	1.5
% of error	3%	0%	2%	0.3%	50%
$A_{min}[dB]$	19.92	22.96	25.1	22.5	22
% of error	0.4%	14.8%	25.5%	12.4%	10%

cumulative distribution functions(CDF) of two samples by assuming that they come from the same distribution or from different distributions and consequently by applying the KS-test to random variables it is possible to determine if they differ significantly [31]. The linear magnitude responses of simulation results with a different software as well as with experimental results were normalized into cumulative spectral energy distributions over the band of interest.Unlike standard point-by-point metrics (e.g., Root-Mean-Square Error), which can obscure localized anomalies through wideband averaging, the KS D-statistic strictly evaluates the maximum supremum divergence in the cumulative spectral topology. This provides a rigorous, non-parametric validation of the filter's shape integrity against unmodeled parasitic deformations.

Fig. 11 shows the histograms and the CDFs of the magnitude responses in the frequency domain of both, the Pascal and the SIW filters. According to the graphs in Fig. 11 (b), the experimental response exhibit a good behavior compared to LTSPICE and SAFIMAM in the case of the Pascal filter. It can be appreciated that a maximum absolute difference between the two more distant points in the CFD of the Pascal filter of 0.0936 was achieved when comparing SAFIMAM and LTSPICE as well as comparing LTSPICE with the FPAA results. On the other hand, a difference of 0.0128 was attained when comparing for the SAFIMAM with the FPAA results. Again, based on the graphs in Fig. 11 (d), the experimental response exhibit a good behavior compared to ADS and SAFIMAM in the case of SIW filter. It can be seen that a maximum absolute difference between the two more distant points in the CFD of the SIW filter of 0.0465 was achieved when comparing SAFIMAM and ADS as well as comparing ADS with the SIW results. Further, a difference of 0.0164 was attained when comparing for the SAFIMAM with ADS. All in all, do not lose sight that inasmuch as the closer the KS statistic of 0 is, the more identical the two distributions being compared are. Therefore, with these outcomes we can conclude that SAFIMAM accuracy is highly reliable.

It is important to compare the results of the Pascal filter synthesized in this work with a Pascal filter synthesized with

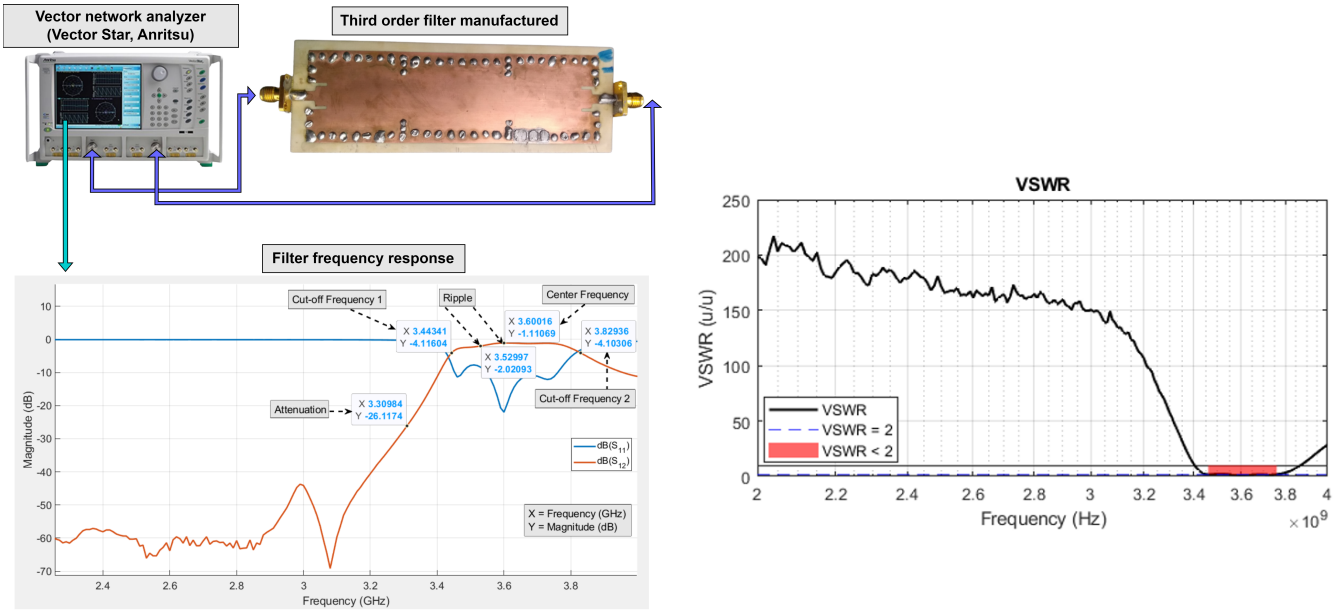

(a) (b)

Fig. 10. Experimental test-setup of SIW filter for 5G: (a) The S_{11} and S_{12} parameters, and (b) the VWSR parameter.

TABLE VII
COMPARISON AMONG DIFFERENT FILTER SYNTHESIS TOOLS INCLUDING SAFIMAM FOR THE SYNTHESIS OF A CHEBYSHEV TYPE I PASSBAND FILTER FOR 5G APPLICATIONS

Simulation Results	SAFIMAM	LC Filter Design Tool	RF Hammer
$f_0[GHz]$	3.625	3.59	3.59
% of error	0.97%	0%	0%
$BW[GHz]$	0.37	0.42	0.39
% of error	5.12%	7.69%	0%
$f_1[GHz]$	3.44	3.38	3.40
% of error	1.17%	0.58%	0%
$f_2[GHz]$	3.81	3.80	3.79
% of error	0.52%	0.26%	0%
$A_{max}[dB]$	1	0.99	1
% of error	0%	1%	0%
$A_{min}[dB]$	25	25.5	28
% of error	0%	2%	12%

different tools. However, there are not tools that allow the synthesis of Pascal filters other than SAFIMAM. Yet, it is still possible to compare the results of SAFIMAM versus different design tools if a Cheby I filter is employed as the circuit under test with the same specifications used for creating the Pascal filter, i.e. a range of frequencies from 50Hz to 3KHz with a center frequency of 1525Hz, an attenuation of 20dB in the stopband, a maximum ripple in the bandpass of 1dB and a transition ratio (ω_s/ω_p) of 2. Thus, taking into account these specifications the results reported in Table VI are achieved.

Table VI shows the parameters of interest of the filter synthesized such as the center frequency, the bandwidth the ripple in the passband and the attenuation in the bandstop. Additionally, it also the percentage of error with respect to the specifications provided for the synthesis labor. Analog filter Wizard and SAFIMAM exhibit a similar performance reaching the best results among all the options. However, in Analog Filter Wizard Pascal approximation is not available. Thus, the scope of SAFIMAM is better than the rest since it allows the synthesis of filters not just by means of classical approximation methods but also through the Pascal approach.

Just as in the previous case, we compare the results of the SIW filter synthesized with SAFIMAM, in its RLC (Cheby I) version, with the results delivered by different tools. In this case, the band of interest ranges from 3.4GHz to 3.79GHz, with a maximum ripple in the passband of 1dB, a minimum attenuation in the stopband of 25dB, and a transition ratio of 2.5. Table VII shows the outcomes produced with their corresponding percentage of error. As can be seen, RF Hammer and SAFIMAM are the tools which exhibit a superior performance with smaller errors for each parameter of interest.

Finally, to validate the functionality of the proposed software, the synthesis of both active and passive filters reported in the third section of this work have been carried out with interesting results. Yet, it is also intriguing to compare the performance of these filters to some others reported in the literature in order to have a broader overview of the feasibility of the synthesized structures. Table VIII shows some important features of both, *EMG* and 5G filters, reported herein and elsewhere. In the case of the EMG application, most of the reported filters are experimentally proved with the exception of [32], where only simulation results are expressed; the performance of the Pascal structure in terms of filter-order, bandwidth and attenuation in the bandstop is competitive when compared to the other works. On the other hand, the performance of the filters for 5G applications found in the literature are also similar to the Chebyshev-type I synthesized with SAFIMAM despite the technological differences in their implementation. Therefore, the synthesized filter structures produced by the proposed software are, at least, feasible and

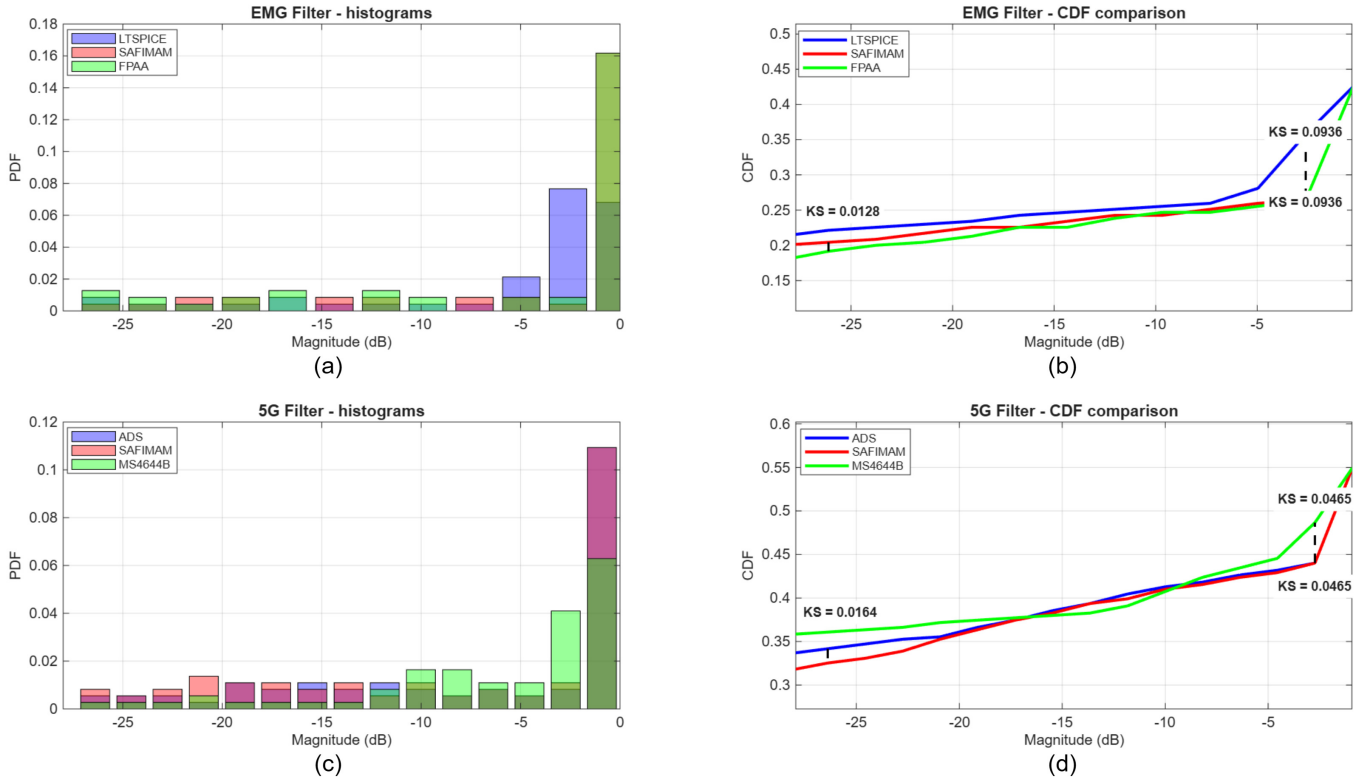

Fig. 11. (a) Histograms of the frequency response of the magnitude of the Pascal filter synthesized (SAFIMAM, LTSPICE and experimental). (b) CDF comparison among the SAFIMAM, LTSPICE and experimental results. (c) Histograms of the frequency response of the magnitude of the 5G filter synthesized (SAFIMAM, ADS and experimental). (b) CDF comparison among the SAFIMAM, ADS and experimental results.

reliable.

V. Conclusions

A MATLAB App Designer *GUI*, called SAFIMAM has been developed. The proposed *GUI* allows the user to calculate at different levels, from top to down, the results concerned to the synthesis of analog filter through any classical approximation method as well as the Pascal approach. Some of the results that can be computed by the *GUI* include: the filter order; the selection of the type of approximation method for the synthesis of the filter; the transfer function generation; the Bode plot; the impedance and frequency denormalizations; the lowpass filter transformation to highpass, bandpass and bandreject filters; the selection of either of the Pascal filters available, the passband optimized and the stopband optimized; and the resistively double terminated *LC* ladder network, in π or T type, of any of the approximations methods employed for the synthesis. All these results can be obtained by providing a few design specifications to the *GUI*: the ripple in the bandpass (A_{max}), the attenuation in the bandstop (A_{min}), the transition ratio (ω_s/ω_p), and the resistance value at the input of the *LC* ladder network, R_S.

Two design examples synthesized with SAFIMAM were implemented, an active Pascal filter optimized in the bandstop for EMG signals, implemented with AN231E04 FPAAs embedded in the Anadigm QuadApex Development Board, and tested in the multi-function instrument *Digilent Analog Discovery 2*, which fulfilled the design specifications of 1dB ripple in the bandpass, 20dB of attenuation in the bandstop, a transition ratio $(\omega_s/\omega_p) = 2$, and a R_S value of 100Ω. The other realization corresponds to a third order Chebyshev type I SIW filter built in a PC board with a Rogers 4003C substrate. Regarding the SIW filter, the experimental test setup was done with an ANRITSU Vector Network Analyzer model MS4644B. Experimental results agree with the results provided by SAFIMAM, whose design specifications for this case were 1dB ripple in the bandpass, 25dB of attenuation in the bandstop, a transition ratio $(\omega_s/\omega_p) = 2.5$, and a R_s value of 50Ω.

It is important to remark that, quantitative metrics regarding computational efficiency such as algorithmic scalability, in the range of milliseconds, and synthesis runtime, in a hundred seconds, prove that the program maintains a good performance as workloads grow without significant slowdowns. Moreover, before prototyping, Monte Carlo tolerance simulation (over 100 runs) for the active Pascal filter was carried to verify its robustness; with a median attenuation at f_1 of -2.89dB and a standard deviation (σ) of 0.25dB, a median (μ) at f_2 of -3.84dB with a σ of 0.27dB, and a μ for attenuation at f_0 of -0.95dB with a σ of 0.13dB, these results demonstrate the feasibility of the proposed EMG active filter. In addition, SAFIMAM and prototype EMG results match well, relative errors of $\approx 2.33\%$ and $\approx 2.4\%$ for f_0, BW and f_1 and f_2 were estimated whereas errors for A_{max} and A_{min} of $\approx 0\%$ and 1.6%, respectively, were assessed. Besides, with an output noise of $\approx 1.69mV_{rms}$, the synthesized and prototyped

TABLE VIII
COMPARISON OF THE IMPLEMENTED FILTERS SYNTHESIZED WITH SAFIMAM WITH SOME OTHER FOR BOTH EMG AND 5G APPLICATIONS, RESPECTIVELY, REPORTED IN THE LITERATURE. REGARDING THE ACRONYMS, WE HAVE: NR = NO REPORTED; NM-BVD=NEW MODIFIED BUTTERWORTH-VAN DYKE; SIW = SUBSTRATE INTEGRATED WAVEGUIDE; GAF = GRAPHEN-ASSEMBLED FILMS; AW= ACOUSTIC WAVE

Parameters	**EMG This work**	**EMG [32]**	**EMG [33]**	**5G This work**	**5G [34]**	**5G [35]**
Filter type	3rd ord.	Biquad	3rd ord.	3rd ord.	NR	NM-BVD
Realization	Pascal Active FPAAs	Active CMOS	Butter Active OPAMPs	Cheby I SIW	GAF	AW
f_0	1525 Hz	1475 Hz	314.65 Hz	3.6 GHz	3.5 GHz	2.593 GHz
BW	2878.64 Hz	2950 Hz	596.7Hz	380 MHz	170 MHz	196MHz
α_{max}	1 dB	0 dB	0dB	0.91dB	NR	0.01dB
α_{min}	20.31 dB	20 dB	24.4 dB	25dB	27dB	30dB

EMG filter exhibits an acceptable noise value for EMG signal processing considering that EMG signals achieved up to $5mV$ voltage swing. On the other hand, the synthesized and prototyped SIW filter also exhibits good experimental results, parameters S_{11} and S_{12} indicate a good match in the band of interest, the quality factor Q is ≈ 9.5, i.e., the filter has a moderate selectivity, meaning that it allows signals to pass through the passband with minimal losses while effectively attenuating signals outside this band. Also, a $VSWR < 2$ between 3.46 GHz and 3.76 GHz was identified, indicating the filter exhibits good impedance matching. As in the previous case, of the Pascal EMG filter realization, the SIW prototyped filter errors regarding the design specifications are low enough to consider the synthesized filter by SAFIMAM a good solution (0.14% error for f_0, 2.6% for BW, 9% for A_{max}, and 0.02% for A_{min}). Finally, accuracy of the two synthesized filters with SAFIMAM, were compared to synthesized filter structures with a different software by means of the KS-test. The results reported in section IV indicate that SAFIMAM accuracy is highly reliable. Furthermore, comparisons of the implemented filters synthesized with SAFIMAM with some other for both EMG and 5G applications, respectively, reported in the literature were made; the performance of the Pascal structure in terms of filter-order, bandwidth and attenuation in the bandstop is competitive when compared to the other works; then again, the performance of the filters for 5G applications found in the literature are also similar to the Chebyshev-type I synthesized with SAFIMAM despite the technological differences in their implementation.Therefore, the synthesized filter structures produced by the proposed software are, at least, feasible and reliable.

Last but not least, despite there are many interesting CAD tools for the synthesis of analog filters, like those widely discussed in section I, most of them employ classic approximation methods mainly, with a few exceptions that incorporate some other approximation methods such as Legendre, Bessel, Gaussian and Linear-Phase. However, to date, the only synthesis tool capable of synthesizing Pascal filters is the one proposed in this work: SAFIMAM. This, in turn, expands the user alternatives of filters whose performance suits in a better form their design needs. In terms of development, SAFIMAM is competitive according to the results of the many different tests applied. Yet, it is bounded to synthesize filters within a a range of order $n \in [2, 21]$.

REFERENCES

[1] L. A. Sánchez-Gaspariano, C. Muñiz-Montero, J. M. Muñoz-Pacheco, C. Sánchez-López, L. C. Gómez-Pavón, A. Luis-Ramos, and A. I. Bautista-Castillo, "CMOS Analog Filter Design for Very High Frequency Applications," in Electronics, vol. 9, no. 2, p. 362, 2020. Doi: 10.3390/electronics9020362.

[2] A. M. Davis, "Approximation," in Passive, Active and Digital Circuits, 3rd ed., W.-K. Chen, Ed. Boca Raton, FL, USA: CRC Press, 2018, pp. 2.1–2.30.

[3] D. Baez-López, Analog Circuits: Applications, Design and Performance, NOVA science publishers, 2012.

[4] S. C. Dutta Roy, "A State-of-the-Art Survey on Linear Phase Digital Filter Design," in Topics in Signal Processing, Singapore: Springer, 2020, pp. 241–264, $doi : 10.1007/978 - 981 - 13 - 9532 - 1\_18$.

[5] M. Sanduleanu and D. Craven, "On broadband, linear-phase, flat group delay, all-pole, low-pass filters for high-speed, data communication," Results in Engineering, vol. 25, p. 104103, Mar. 2025, doi: 10.1016/j.rineng.2025.104103.

[6] A. Kumar and A. K. Verma, "Comparative performance of some polynomial-based lowpass filters for microwave/digital transmission applications," International Journal of Electronics, vol. 106, no. 1, pp. 13–35, 2019, doi: 10.1080/00207217.2018.1494338.

[7] G. Fedele and Andrea Ferrise, "Explicit solution of the finite time L2-norm polynomial approximation problem," Applied Mathematics and Computation, vol. 217, no. 21, pp. 8354–8359, Jul. 2011, doi: 10.1016/j.amc.2011.03.032.

[8] W. Ngamkham, C. Sawigun, S. Hiseni and W. A. Serdijn, "Analog complex gammatone filter for cochlear implant channels," Proceedings of 2010 IEEE International Symposium on Circuits and Systems, Paris, France, 2010, pp. 969-972. Doi: 10.1109/ISCAS.2010.5537383.

[9] T. J. Goodman and M. F. Aburdene, "Pascal filters," in IEEE Transactions on Circuits and Systems I: Regular Papers, vol. 55, no. 10, pp. 3090–3094, 2008, doi: 10.1109/TCSI.2008.925374.

[10] G. B. Kasapoglu, E. A. Karagianni, M. E. Fafalios, and I. A. Koukos, "Coefficients calculation in Pascal approximation for passive filter design," in Computation, vol. 6, no. 1, p. 18, 2018, doi: 10.3390/computation6010018.
[11] Marki Microwave, "LC filter design tool." [Online]. Available: https://markimicrowave.com/technical-resources/tools/lc-filter-design-tool/ [Accessed: Mar. 12, 2026].
[12] Texas Instruments, "WEBENCH Filter Designer basics." [Online]. Available: https://www.ti.com.cn/content/dam/videos/external-videos/en-us/1/3816841626001/5094691843001.mp4/subassets/filter-designer-presentation.pdf [Accessed: Mar. 12, 2026].
[13] Analog Devices, "Filter design tool — Filter Wizard." [Online]. Available: https://tools.analog.com/en/filterwizard/ [Accessed: Mar. 12, 2026].
[14] G. Marinova, O. Chikov, and B. Rodic, "E-content and tool selection in the cloud-based online-cadcom platform for computer-aided design in communications," in Proc. 2019 15th International Conference on Telecommunications (ConTEL), 2019, pp. 1–5, doi: 10.1109/ConTEL.2019.8848537.
[15] Microchip Technology, "FilterLab active filter designer." [Online]. Available: https://filterlab.microchip.com/filter [Accessed: Mar. 12, 2026].
[16] Analog Devices, "FilterCAD designs filters quickly and easily." [Online]. Available: https://www.analog.com/en/resources/design-notes/free-filtercad-designs-filters-quickly-and-easily.html [Accessed: Mar. 17, 2026].
[17] Texas Instruments, "FilterPro." [Online]. Available: https://www.ti.com/lit/an/sbfa001c/sbfa001c.pdf [Accessed: Mar. 18, 2026].
[18] Softpedia, "Filter Wiz Lite." [Online]. Available: https://www.softpedia.com/get/Science-CAD/Filter-Wiz-Lite.shtml [Accessed: Mar. 18, 2026].
[19] Coilcraft, "Coilcraft LC filter designer software." [Online]. Available: https://www.coilcraft.com/en-us/other/coilcraft-lc-filter-designer-software/ [Accessed: Mar. 18, 2026].
[20] RFHammer, "RF Filter," 2026. [Online]. Available: https://www.rfhammer.com [Accessed: Mar. 12, 2026].
[21] G. Çakir, S. Gündüz, and L. Sevgi, "A Matlab-based Filter Design Tool Using the Analogy between Wave and Circuit Theories," in Brain-Inspired IT III (International Congress Series), vol. 1291, pp. 141–148, Elsevier, 2006, doi: 10.1016/j.ics.2006.03.042.
[22] MathWorks, "Filter Designer." [Online]. Available: https://la.mathworks.com/help/signal/ug/introduction-to-filter-designer.html [Accessed: Mar. 18, 2026]
[23] L. Huelsman, "Filterd-mathcad worksheets for analog filter design," IEEE Circuits and Devices Magazine, vol. 17, no. 3, pp. 4–5, 2001.
[24] Elsie Software, "Elsie." [Online]. Available: https://elsie.apponic.com/ [Accessed: Mar. 18, 2026].
[25] H. G. Dimopoulos, "Even-order passive filters: Pascal versus Chebyshev", *International Journal Of Circuit Theory And Applications*. vol. 41, pp. 946-959, 2013.
[26] H. G. Dimopoulos, Analog Electronic Filters: Theory, Design and Synthesis. Dordrecht: Springer Science & Business Media, 2011, doi: 10.1007/978-94-007-2190-6.
[27] P. Podder, H. Mehedi, I. Rafiqul, and S. Mursalin, "Design and implementation of Butterworth, Chebyshev-I and elliptic filter for speech signal analysis," in arXiv [eess.SP], 2020, doi: 10.48550/arXiv.2002.03130.
[28] M. K. Adimulam and M. B. Srinivas, "Modeling of EXG (ECG, EMG and EEG) non-idealities using MATLAB," 2016 9th International Congress on Image and Signal Processing, BioMedical Engineering and Informatics (CISP-BMEI), Datong, China, 2016, pp. 1584-1589, doi: 10.1109/CISP-BMEI.2016.7852968.
[29] GSMA, "Espectro 5G: Posición de política pública de la GSMA," 2019. [Online]. Available: https://www.gsma.com/spectrum/wp-content/uploads/2019/10/5G-Spectrum-Positions-SPA.pdf. [Accessed: Mar. 22, 2023].
[30] L. H. Ruiz, "Sistema antena-filtro pasa banda en tecnología SIW centrado a 3.6 GHz para 5G," Ph.D. dissertation, Benemérita Universidad Autónoma de Puebla, 2021.
[31] C. Sánchez-López et.al., "Accuracy vs simulation speed trade-off enhancements in the generation of chaotic attractors," 2013 IEEE 4th Latin American Symposium on Circuits and Systems (LASCAS), Cusco, Peru, 2013, pp. 1-4, doi: 10.1109/LASCAS.2013.6518988.
[32] C. Muñiz-Montero, L. H. Salas-Barradas, L. A. Sánchez-Gaspariano, and A. Díaz-Sánchez, "A 25nA, 66.95dB dynamic range CMOS tunable filter for EEG, ECG and EMG measurements," in Proc. IEEE International Autumn Meeting on Power, Electronics and Computing (ROPEC), Ixtapa, Mexico, 2015, pp. 1–5, doi: 10.1109/ROPEC.2015.7395116.
[33] M. Z. Jamal, D. -H. Lee and D. J. Hyun, "Real Time Adaptive Filter based EMG Signal Processing and Instrumentation Scheme for Robust Signal Acquisition Using Dry EMG Electrodes," 2019 16th International Conference on Ubiquitous Robots (UR), Jeju, Korea (South), 2019, pp. 683-688, doi: 10.1109/URAI.2019.8768662.
[34] Y. Hui, R. Song and D. He, "Filtering Antenna Array based to Graphene-Assembled Films for 5G Applications," 2022 IEEE MTT-S International Wireless Symposium (IWS), Harbin, China, 2022, pp. 1-3, doi: 10.1109/IWS55252.2022.9978149.
[35] Y. Jang and D. Ahn, "Analyzing three types of design methods for 5G N41 band acoustic wave filters," Int. J. RF Microw. Comput. Aided Eng., 2024, doi: 10.1155/2024/4638443.

Víctor H. Hernández-Juárez received the MSc and the BSc degree, both in Electronics, from the Benemérita Universidad Autónoma de Puebla (BUAP), and Instituto Politécnico Nacional, respectively. His research interests include both analog and digital signal processing, coding, radio communications systems and networks design. Currently, he is pursuing the PhD degree from BUAP, his research topic focuses on the synthesis and design of analog filters for biomedical applications.

Luis A. Sánchez-Gaspariano received the PhD degree in Electronics from INAOE, Puebla, México, in 2011. During 2009 he was a visiting scholar in the Integrated Circuits Design (ICD) group at the University of Twente, in the Netherlands. He is currently with the Electronics Faculty at Benemérita Universidad Autónoma de Puebla (BUAP), in Puebla, México, as a full professor. His research interests include the development of Electronic Design Automation (EDA) tools and the development of electronic automotive systems.

Carlos Sánchez-López received his Ph.D. degree in Electronics from INAOE, México in 2006. Since January 2006, he is with the Universidad Autónoma de Tlaxcala (UAT) in Apizaco, México, as an Associate Professor and Researcher. Dr. Sánchez-López is the author and coauthor of book chapters, research journal papers, and international conference proceedings in the fields of modeling and simulation of linear and nonlinear circuits and systems, chaotic oscillators, symbolic analysis, mixed-signal circuits, RF circuits, and computer-aided circuit design.

Richard Torrealba-Meléndez received the Ph.D degree from INAOE, México in 2014. He is currently a full Professor-Researcher with the Electronics Faculty at the Benemérita Universidad Autónoma de Puebla. Dr. Torrealba is a regular member of the Sistema Nacional de Investigadores (SNI) de México, a top level program of the government of México. His research interests include: antenna design, wireless personal communications, dielectric spectroscopy at microwave frequencies and telecommunications.

Jesús M. Muñoz-Pacheco is a tenured professor in the Electronics Faculty at Benemérita Universidad Autónoma de Puebla, México. Dr. Muñoz-Pacheco founded and leads the research group: Fractional-order Systems and Nonlinear Circuits. He has published about 120 scientific works related to chaotic systems and fractional-order calculus. Dr. Muñoz-Pacheco is Associate Editor for Frontiers in Physics, IJNM-Wiley, Frontiers in Applied Mathematics and Statistics, Chaos Theory and Applications, etc.

Carlos Muñiz-Montero received his Ph.D. degree in Electronics from INAOE, México, in 2008. He has authored and co-authored several books, book chapters, journal articles, and conference papers. Since 2012, he has been an Associate Professor in the Department of Electronics and Telecommunications Engineering at Universidad Politécnica de Puebla (UPPue), where he has led the Electronics Group since 2017. His research interests include analog, mixed-signal, RF electronics, control systems, and fractional-order systems.

Luz del Carmen Gómez-Pavón received her Ph.D. degree from the Benemérita Universidad Autónoma de Puebla, México, in 2001. She is a regular member (level-2) of the National System for Researchers, from México. Her research interests include optical fiber-based lasers systems, specially integration of nanotechnology in optical laser sources. Instrumentation of photonic devices, and their related applications.